ELSEVIER

Journal of Pharmaceutical and Biomedical Analysis
26 (2001) 463–476

JOURNAL OF
PHARMACEUTICAL
AND BIOMEDICAL
ANALYSIS

www.elsevier.com/locate/jpba

NMR of biofluids and pattern recognition: assessing the impact of NMR parameters on the principal component analysis of urine from rat and mouse

Barbara C.M. Potts [a,*], Alan J. Deese [a], Gregory J. Stevens [b], Michael D. Reily [c], Donald G. Robertson [d], Jeffrey Theiss [b]

[a] *Department of Analytical Chemistry, Agouron Pharmaceuticals, Inc., A Pfizer Company, 3565 General Atomics Court, San Diego, CA 92121, USA*

[b] *Department of Toxicology, Agouron Pharmaceuticals, Inc., A Pfizer Company, 3565 General Atomics Court, San Diego, CA 92121, USA*

[c] *Department of Discovery Technologies, Pfizer Global Research & Development, Ann Arbor Laboratories, 2800 Plymouth Road, Ann Arbor, MI 48106-1047, USA*

[d] *Department of Worldwide Preclinical Safety, Pfizer Global Research & Development, Ann Arbor Laboratories, 2800 Plymouth Road, Ann Arbor, MI 48106-1047, USA*

Received 31 October 2000; received in revised form 8 February 2001; accepted 22 February 2001

Abstract

The ability to interpret metabolic responses to toxic insult as expressed in altered urine composition and measured by NMR spectroscopy is dependent upon a database of proton NMR spectra of urine collected from both control and treated animals. Pattern recognition techniques, such as principal component analysis (PCA), can be used to establish whether the spectral data cluster according to a dose response. However, PCA will be sensitive to other variables that might exist in the data, such as those arising from the NMR instrument itself. Thus, studies were conducted to determine the impact that NMR-related variables might impart on the data, with a view towards understanding and minimizing variables that could interfere with the interpretation of a biological effect. This study has focused on solvent suppression methods, as well as instrument-to-instrument variability, including field strength. The magnitude of the NMR-induced variability was assessed in the presence of an established response to the nephrotoxin bromoethanamine. Changes caused by the model toxin were larger and easily distinguished from those caused by using different solvent suppression methods and field strengths.

Keywords: Metabonomics; Biofluid NMR spectroscopy; Principal component analysis; Pattern recognition; Solvent suppression; Urine

* Corresponding author. Present address: Suite 210, Nereus Pharmaceuticals, Inc., 9393 Towne Centre Drive, San Diego, CA 92121, USA. Tel.: +1-858-5874090; fax: +1-858-5874088.

E-mail address: bpotts@nereuspharm.com (B.C.M. Potts).

0731-7085/01/$ - see front matter
PII: S0731-7085(01)00430-7

1. Introduction

The application of ^{1}H NMR spectroscopy to the study of the metabolic composition of biofluids, coupled with pattern recognition to classify the NMR-generated data has led, in part, to a 'metabonomic' approach to toxicological assessment [1]. Metabonomics involves the measurement of the dynamic metabolic response of an organism to xenobiotic pressure. Such pressure, which may be applied by exposure to a drug candidate substance or by toxic insult, alters the ratios and concentrations of endogenous biochemicals in cells and tissues and ultimately results in modified biofluid compositions. Furthermore, reports that various classes of toxin produce characteristic changes in the patterns of endogenous metabolites in biofluids suggest that information on the sites and mechanisms of toxicity may be obtained by monitoring these changes. The metabonomic approach thus offers a means of assessing in vivo multiorgan integrity over time in response to xenobiotic stimuli and has potential applications in drug safety assessment during the drug discovery process [1,2].

The ability to interpret metabolic responses that are expressed in altered urine composition using NMR spectroscopy is dependent upon a database of ^{1}H NMR spectra of urine collected from both control and treated animals. The analysis of large numbers of complex NMR spectra can be managed through data reduction and pattern recognition techniques [3,4], such as principal component analysis (PCA) [5]. The principal components (PCs) are linear combinations of the original input descriptors (in this case, integrals obtained from a series of urine ^{1}H NMR spectra) with appropriate weighting coefficients, such that the first PC contains the greatest amount of variance in the data and subsequent PCs contain lesser amounts of variance. By plotting only the first two or three PCs, the original N-dimensional data (in which each dimension represents an integral region) are effectively compressed into two or three manageable dimensions. The resulting PC maps can be used to visualize any clustering patterns associated with a metabolic response [1]. However, a PCA will also be inherently sensitive to other variables that might exist in the data. In fact, the NMR instrument itself is a potential source of variation between spectra that might be detected in a PCA. This warranted an investigation of the impact of NMR experimental variables on principal component urinalysis.

The focus of this study is on solvent suppression methods, field strength, and reproducibility across instruments. The latter issues are potentially problematic in cases where pooling or comparing NMR spectra from more than one instrument is being considered; the utility and relevance of the data become dependent upon the consistency across the instruments used in the data collection. The selection of a solvent suppression scheme is of broader concern, since suppression of the large water resonance that dominates the NMR spectrum of urine is required in all cases in order to increase the dynamic range and enable the detection and quantification of low level metabolites. Numerous solvent suppression methods have been proposed for urinalysis [6], including simple presaturation (e.g. [7]); the Hahn spin-echo (e.g. [8,9]), 1D-NOESY with presaturation (e.g. [10]), and Watergate [11]. Each sequence has unique characteristics in terms of selectivity, excitation profile, attenuation of exchangeable proton resonances, and resulting baseline and phase distortions. These unique profiles provide a potential source of variability across spectra that might compete with the interpretation of the treatment related effect that is the object of the analysis. Thus, we have sought to establish the impact that solvent suppression and instrument-to-instrument variability might impart on the data, with a view towards understanding and minimizing the variables that might interfere with the interpretation of a biological effect. The impact of line-broadening, phasing, and selection of descriptors have been described by others [4].

2. Experimental

2.1. Mouse urine collection and sample preparation

A total of six male B6C3F1 mice (20–25 g) from Charles River (Kansas City, MO) were used

in this study. Animals were housed in metabolism cages (one animal per cage), with free access to food and water under controlled conditions (temperature, humidity, and a 12 h light–dark cycle). Urine samples were collected into conical tubes over dry ice containing 1.0 ml aqueous sodium azide (1.0% w/v) at 24 h intervals over a period of seven days. The samples were stored at −20°C until they were prepared for NMR analysis. After thawing, day 2 mouse urine samples were diluted 2:1 urine:buffer (0.2 M sodium phosphate, pH 7.4) to minimize pH variations. Additionally, 8.3% (v/v) of 2,2′,3,3′-deuterotrimethylsilylpropionic acid (TSP) in D_2O (11 mM) was added to a final concentration of 0.9 mM to provide an internal chemical shift reference and frequency lock, respectively. Solutions were transferred to 5 mm Wilmad 528 NMR tubes for analysis.

2.2. Rat urine collection and sample preparation

Animal handling, urine sample collection and preparation have been described elsewhere [12]. Sample preparation involved dilution of urine with 200 mM phosphate buffer. Prior to dilution with buffer, the pH of the urine samples ranged from 6.0 to 8.0 ($\pm$0.5 pH unit). The pH was not measured immediately after dilution with 200 mM phosphate buffer, which generally normalizes the pH to a range from 6.7 to 7.6 [6], but a random pH sampling was performed after NMR analysis at 500 MHz (vide infra). After NMR analysis at 600 MHz (vide infra; [12]), the urine samples were stored at −20°C in 96-well plates for a period of 11 months. Samples were then thawed and transferred to 5 mm Wilmad 528 NMR tubes for further NMR analysis at 500 MHz. Samples were then frozen at −80°C for two weeks, after which they were thawed for a second analysis at 500 MHz. The pH was subsequently measured on five random NMR samples using a pH meter and was found to range from 7.10 to 7.41.

2.3. NMR analysis of mouse urines

^{1}H NMR data were collected on a Bruker DRX 500 MHz instrument running XWINNMR V.2.6 and equipped with a ^{1}H-{^{13}C} BBI probe with x,y,z-gradients. Spectra were acquired using 128 scans and 32 K complex points. A total relaxation delay of 1.5 s was used. A spectral width of 9259 Hz resulted in FID acquisition time of 3.539 s. Six unique NMR spectra were acquired on each sample using the following pulse sequences: WET, Watergate, presaturation, and NOESY-presaturation with three unique NOESY-mixing times (10 μs, 100 ms, and 150 ms). For presaturation experiments, each FID was induced using a nonselective 90 degree excitation pulse following a selective soft pulse set on the water resonance during the relaxation delay. For the NOESY-presaturation experiments, presaturation was also employed during the NOESY mixing period. All acquisitions were initiated with four dummy scans, except for the WET sequence, which was initiated with 32 dummy scans. The WET sequence described by Smallcombe and co-workers [13] was used with minor modifications. For the selective WET RF pulses, a SINC shape defined by 1K points was used and applied directly to the water resonance. The tip angles were 81.4, 101.4, 69.3, and 161.0° (T_1 and B_1 insensitive WET sequence) relative to a 20 ms SINC 90° pulse. The gradient pulses were 2 ms in duration and had amplitudes of 60, 30, 15, and 7.5 G/cm. A delay of 250 μs was added before the next RF pulse to allow for gradient recovery. The Watergate pulse sequence was used as described by Sklenar and co-workers [14]. The delay for binomial water suppression was set to 150 μs. The gradient pulses were 2 ms in duration and had amplitudes of 14 G/cm. The final 90° pulse in the binomial sequence was finely adjusted to give the best phasing of the residual water resonance.

2.4. NMR analyses of rat urines

2.4.1. Analysis at 600 MHz

NMR analysis (600 MHz) of the rat urine samples has been described elsewhere [12] but parameters are summarized herein for direct com vparison with 500 MHz parameters. NMR free induction decays (FIDs) were acquired on a Varian Inova 600 running VNMR software ver-

sion 6.1B and equipped with a ^{1}H-{^{15}N, ^{13}C} flow cell (120 μl active volume) and Varian automated sample transport (VAST) accessory. Using the VAST accessory, a total of 520 μl of the prepared urine samples was withdrawn from either foil-sealed polypropylene 96 deep-well plates or 2 ml septum-capped glass vials and pumped into the flow cell. Two complete cell washes with an approximately isotonic phosphate buffer were performed between each sample injection. Final spectra were accumulations of 64 individual FIDs. Each FID was induced using a nonselective 90 degree excitation pulse following a selective soft pulse (1.5 s) set on the water resonance and digitized into 32 K complex data points. A total inter-excitation pulse delay of 3.0 s was used, and was initiated by sequential 1 ms x and y trim pulses to destroy residual transverse magnetization. A spectral sweep width of 6982.6 Hz resulted in an FID acquisition time of 4.679 s for a total recycle time of 7.7 s. The probe temperature was ambient.

2.4.2. Analysis at 500 MHz

Data acquisition at 500 MHz was similar to that described for mouse urinalysis, with the following exceptions. A spectral width of 7002.8 Hz (14.002 ppm) was employed, which resulted in FID acquisition time of 4.679 s, identical to that used at 600 MHz. For presaturation experiments, the relaxation delay was set to 3 s (including 1.5 s for presaturation), giving a total recycle time of 7.68 s. For Watergate, the binomial 90° pulse width was set to 30 μs. The probe temperature was maintained at 26°C. A single sample was subsequently analyzed by variable temperature NMR (21–27°C).

2.5. NMR data processing and principal component analysis

Varian 600 MHz NMR data were transferred to a Silicon Graphics Indigo workstation and converted to Bruker format using XWINNMR (V2.5, Bruker Instruments). All other 500 and 600 MHz NMR data processing was performed using XWINNMR V2.6 on an SGI O2 workstation. FIDs were multiplied by an exponential decay function (LB = 1.0 Hz). Mouse urine spectra were zero filled to 64 K prior to fast Fourier transformation (FFT); rat urine spectra were not zero filled. FIDs were converted to frequency domain spectra using fast Fourier transformation. The resulting spectra were individually phased and baseline corrected; 600 MHz spectra were subjected to polynomial baseline correction using the BASL routine in XWINNMR, while 500 MHz spectra were adjusted for DC-offset correction only. All spectra were referenced to TSP at 0.000 ppm. Data reduction was performed using AMIX software (V2.8, Bruker Instruments). Integrals were measured over 0.04 ppm contiguous regions of the spectrum. Regions devoid of endogenous peaks at either end of the spectrum and the region containing urea and water resonances were excluded from the data reduction. Specifically, mouse urine spectra were integrated from 10.00 to 0.20 ppm, excluding the region from 6.28 to 4.52 ppm. Rat urine spectra were integrated from 10.00 to 0.16 ppm, excluding the region from 6.32 to 4.48 ppm. Rat urine spectra were subsequently integrated over 0.07 ppm segment widths (10.01–0.21 ppm, excluding the region from 6.30 to 4.48 ppm). All data were normalized in AMIX by dividing each integrated segment by the total area of the spectrum (minus the excluded region). The resulting integrals served as input descriptors for principal component analysis and were output into ASCII file format for this purpose. The ASCII files were imported into Microsoft Excel (Microsoft Corporation) before performing principal component analysis using Pirouette (V2.7, InfoMetrix, Inc., Woodenville, WA, USA) Multivariate Data Analysis software.

2.6. NMR simulation of citrate resonances

The NMR spectrum of citrate was simulated at 500 and 600 MHz using the NMR-SIM routine in XWINNMR V2.6. The $\Delta\delta$ between citrate methylene proton resonances was set to 0.14 ppm, a typical value observed in the urine spectra in this study. ^{2}J was set to 15.6 Hz. The resulting FIDs

were multiplied by an exponential decay function (LB = 2.5 Hz) prior to Fourier transform to approximate the citrate linewidths observed in the urine spectra. The spectra resulting from these simulated FIDs were reduced by integration over 0.04 ppm contiguous regions using AMIX (V2.8, Bruker Instruments).

3. Results and discussion

The effect of solvent suppression on the principal component analysis of urine NMR spectra was explored during the course of feasibility studies in the mouse, a species that has not been previously represented in literature-documented NMR-pattern recognition studies. Mouse urines were analyzed by NMR spectroscopy at 500 MHz using four basic solvent suppression schemes, Watergate [14], WET [13], presaturation, and NOESY-presaturation, which was expanded to include three NOESY mixing times, 10 μs, 100 ms, and 150 ms. After phasing and baseline correction, regions of each spectrum containing water and urea (6.3–4.5 ppm, the 'excluded region') were removed to eliminate the variable integral intensities associated with these signals [10]. Thereafter, each spectrum was integrated across contiguous regions of equal spectral width to generate input descriptors for principal component analysis. The resulting principal component (PC) map (Fig. 1a) was resolved by solvent suppression scheme in PC1, and by animal in PC2. The greatest stratification occurred among the three major solvent suppression schemes, Watergate, WET, and the presaturation experiments. The latter data were further resolved according to a consistent pattern, with presaturation resolved from NOESY-presaturation, and NOESY-presaturation data resolved according to mixing time.

The source of the solvent suppression-induced variance was explored by analysis of the raw NMR data, the loadings (which represent the relative contributions of each input descriptor to the principal component of interest), and spectral reconstructions generated from the input descriptors (segment integrals). In order to simplify the analysis, the mouse data set was limited to consider only the PC1 extremes, the Watergate and presaturation data. PCA of this limited data set resulted in the expected resolution in PC1. The corresponding loadings were weighted with negative values in the region from $\sim$3.3 to 4.3 ppm, just upfield of the excluded region. Analysis of the reconstructed data (Fig. 1b) indicated that this region was attenuated in the Watergate spectra. This effect is attributed to differences in the baselines around the water signal and to the null at the water resonance produced by the Watergate 3-9-19 sequence, which is not sufficiently narrow to preclude attenuation of neighboring protons [11]. Comparative analysis of the original NMR data confirmed the expected attenuation of signals just upfield of the water resonance in the Watergate spectra. The signals immediately downfield of water must be similarly attenuated, however, this effect is obscured by the large urea signal that persists in the Watergate spectra (but which is mostly cut out of the spectra before PCA). The urea signal continues to tail off well beyond 6.3 ppm (downfield of the excluded region), contributing to the overall intensity and elevated baseline in this region. Conversely, the urea signal is well attenuated in the presaturation experiment. Thus, the loadings reveal a positive offset beginning just downfield of the excluded region that diminishes with increasing frequency, reflecting the elevated intensity of this region in the Watergate spectra and the reduced intensity in this region of the presaturation spectra. Interestingly, the WET data were juxtaposed between the presaturation and Watergate data, both in the PCA map (Fig. 1a) and in the spectral reconstructions (data not shown). This is consistent with features that are intermediate between those of the Watergate and presaturation; the urea signal was largely unattenuated, as in Watergate, but the signals just upfield of the water resonance were of comparable intensity to those observed with presaturation. The overall baseline achieved with WET fell between those of the other two solvent suppression schemes. Finally, contributions from differential attenuation of exchangeable protons were considered. While it was possible to identify a number of broad resonances for which the intensities were reduced in the presaturation spectra, the loadings

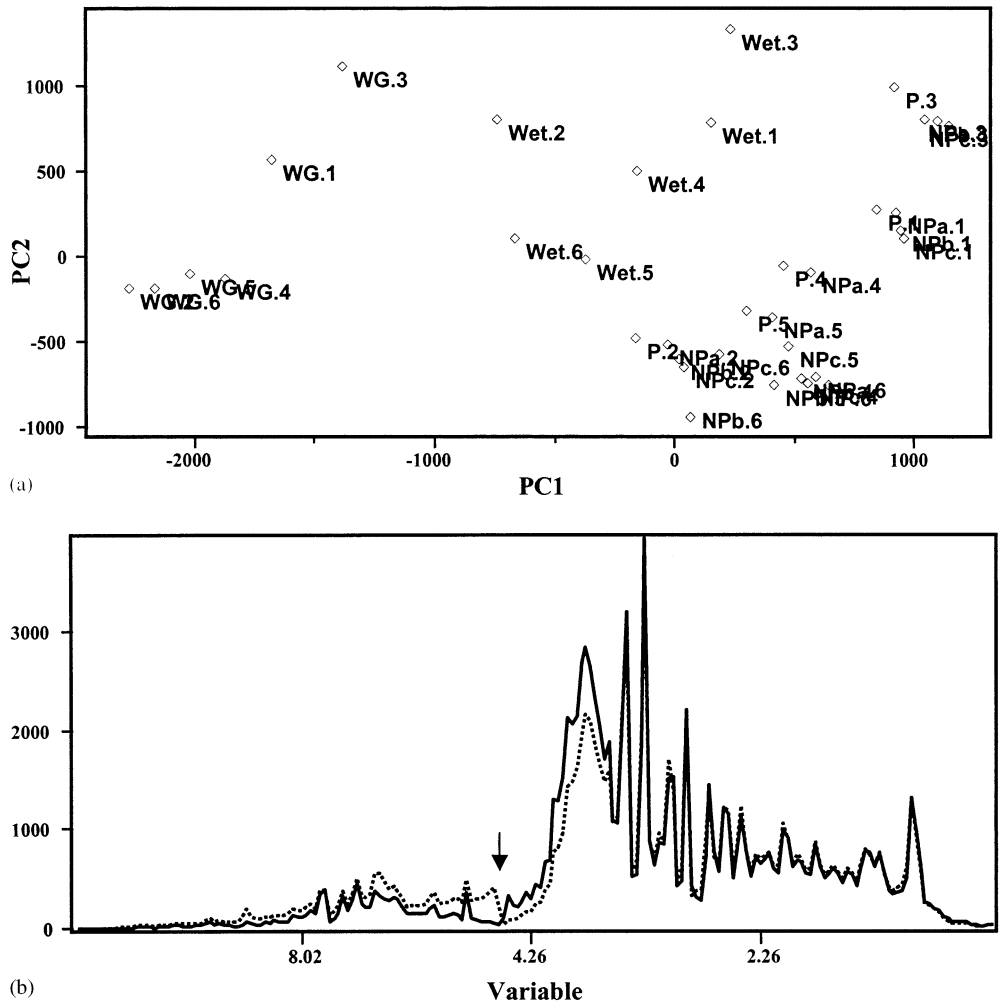

Fig. 1. (a) PC map (mean-centered) of six mouse urine NMR spectra acquired using six different solvent suppression schemes. Data points are denoted by solvent suppression scheme (WG (Watergate); Wet, P (presaturation), NPa (NOESY-presaturation, 10 μs mixing time); NPb (NOESY-presaturation, 100 ms mixing time); NPc (NOESY-presaturation, 150 ms mixing time)) and animal identification number (1–6). (b) Spectral reconstructions generated from the input descriptors (segment integrals, denoted here as 'variables') for Watergate (dotted lines) and presaturation (solid line) spectra. Arrows indicate excluded region. A single pair of reconstructed urine spectra are shown for clarity.

suggested that the variable attenuation of urea and its contribution to the baseline was the dominant effect in the downfield region. Nevertheless, PCA was performed exclusively on the upfield region of the spectra (4.24–0.04 ppm). The resulting PC map (data not shown) was nearly identical to that obtained for analysis of full spectra, further suggesting that differential attenuation of exchangeable protons was not an appreciable source of variance in the data. In summary, the dominant factors contributing to PCA resolution according to solvent suppression scheme were variations in baseline and differential attenuation of resonances near water.

Although it was clearly possible to resolve NMR spectra according to solvent suppression scheme using PCA, of primary interest is the magnitude of this effect relative to a drug response. The impact of solvent suppression was evaluated in the context of the established re-

sponse of rats to the nephrotoxin bromoethanamine (BEA). This system is a reasonable candidate for evaluating relative NMR effects since it has previously served as the subject of study using NMR and pattern recognition methods [7,12]. Briefly, PC maps of rat urine 600 MHz NMR spectra revealed a time- and dose-dependent response to BEA, with low dose urines clustering among predose samples and high dose urines clustering according to sampling day; the greatest distance from predose occurred on days 1 and 2, with incremental movement towards predose on days 3–10 [12]. The physiological implications of these observations have been described elsewhere [7,12]. In order to establish the relative impact of solvent suppression to drug response, the urine samples representing the PC extremes (predose and urines from days 1 and 2) were analyzed at 500 MHz using both presaturation and Watergate for solvent suppression. Each data set gave rise to a comparable PC map to that achieved at 600 MHz. Having established the reproducibility of this pattern over the three NMR data sets (presaturation at 600 MHz; presaturation at 500 MHz, and Watergate at 500 MHz), the relative impact of the NMR parameters was examined by pooling these data and performing principal component analysis with mean-centering (Fig. 2a and b) and autoscaling (Fig. 2c). By including the original 600 MHz data set in this comparative analysis, the solvent suppression study was effectively extended to consider the reproducibility of data collected on another instrument and at higher field strength. The apparent dose response pattern was reproduced by the pooled data, with the high dose samples separated in PC2 by animal and by time point (Fig. 2a). Solvent suppression and field strength had minimal resolving power in the mean-centered PC1/PC2 map (Fig. 2a), however, the three data sets were well resolved in PC3 (Fig. 2b). It was also possible to discriminate between data sets in the autoscaled PC1/PC2 map (Fig. 2c), as this method of analysis does not disfavor small features of the spectra (vide infra).

Spectral reconstructions generated from the input descriptors revealed baseline offsets among the three data sets (Fig. 2d), which were resolved according to the same trend as observed in PC3. The baseline patterns for the two 500 MHz data sets were comparable to those described for mouse urine Watergate and presaturation data (vide supra), while baselines for the 600 MHz spectra were slightly offset from the 500 MHz presaturation spectra. This suggested that baseline was a significant factor contributing to resolution between data sets. However, examination of line plots of the loadings indicated that citrate made appreciable contributions to variability across samples in PC1–3. The analysis of citrate was complicated by several factors. (i) Citrate concentrations varied with dose and time. Reductions in citrate levels in response to BEA have been reported previously [12]. (ii) Citrate chemical shifts were inconsistent across urine samples. The chemical shift variability of citrate might be attributed to the differences in metal ion concentrations among samples, particularly divalent cations that bind to citrate, or to differences in sample pH. Although the addition of 200 mM phosphate buffer, as employed in this study, is expected to normalize the urine pH to a range of 6.7–7.6, citrate has been reported to show chemical shift variations over this range [6]. While integration of each spectrum over a series of contiguous segments of equal and sufficiently large spectral width might compensate for some chemical shift variability [4], the segment width employed in this study (0.04 ppm) was insufficient to counter this effect for citrate. In this study, the chemical shift of the citrate downfield doublet varied by as much as 0.02 ppm, i.e. one half of a segment width, while the upfield doublet exhibited less chemical shift variability ($\Delta\delta_{max} = 0.008$ ppm, or 20% of a segment width). Application of larger segment widths is discussed below. (iii) Citrate chemical shifts varied between the 500 and 600 MHz data sets (Fig. 3a). This variation could be attributed to changes in sample pH or metal ion concentrations that occurred between the two analyses, which were separated by an extended freeze–thaw cycle (vide infra). (iv) Citrate gave rise to a subtle field strength-dependent effect of comparable magnitude to the chemical shift variability between data sets. Although most of the small molecules present in urine give rise to first order

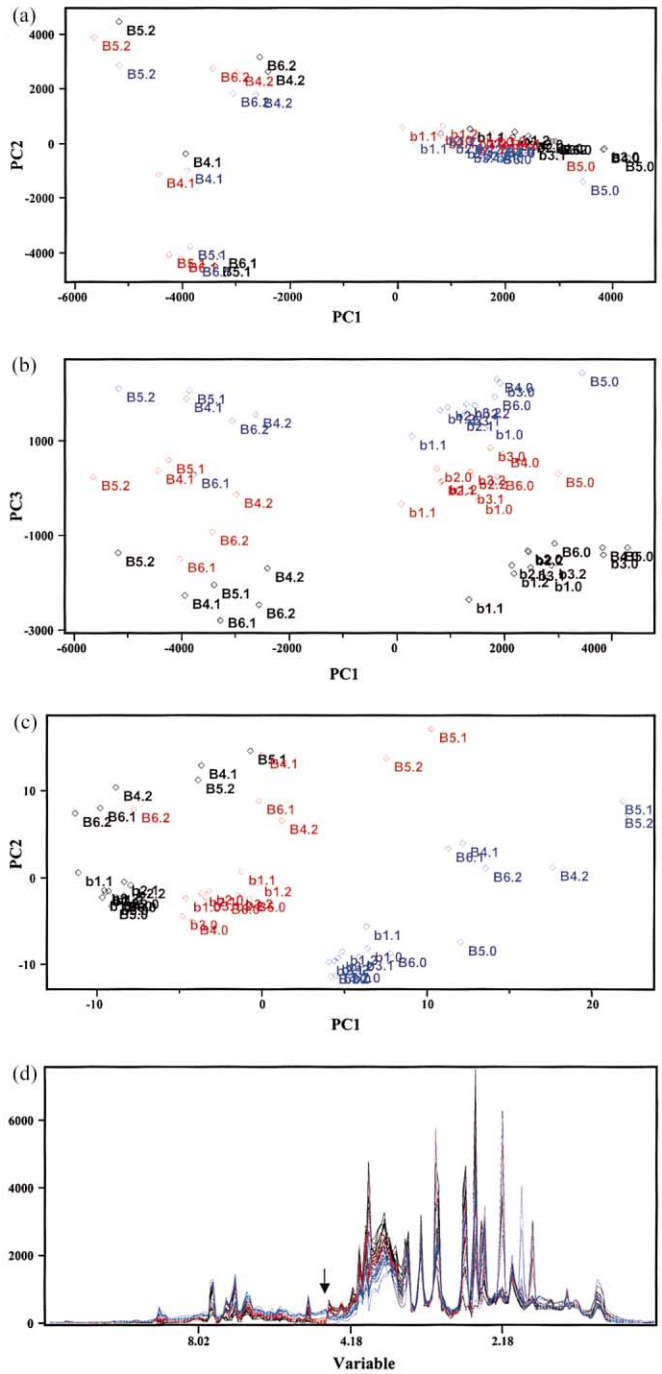

Fig. 2. PC maps ((a,b) mean-centered; (c) autoscaled) of rat urine NMR spectra collected before and after dosing with BEA. Samples are denoted as follows: Dose(B/b)/Animal(# 1–6).Time(0–2); b, low dose (15 mg/kg) BEA; B, high dose (150 mg/kg) BEA; time before (0) and after dosing is given in days. Each NMR data set is identified by a unique color (600 MHz presaturation (black), 500 MHz presaturation (red) and 500 MHz Watergate (blue)). (d) Spectral reconstructions generated from the input descriptors (same color scheme as in (a)–(c)). Arrow denotes excluded region.

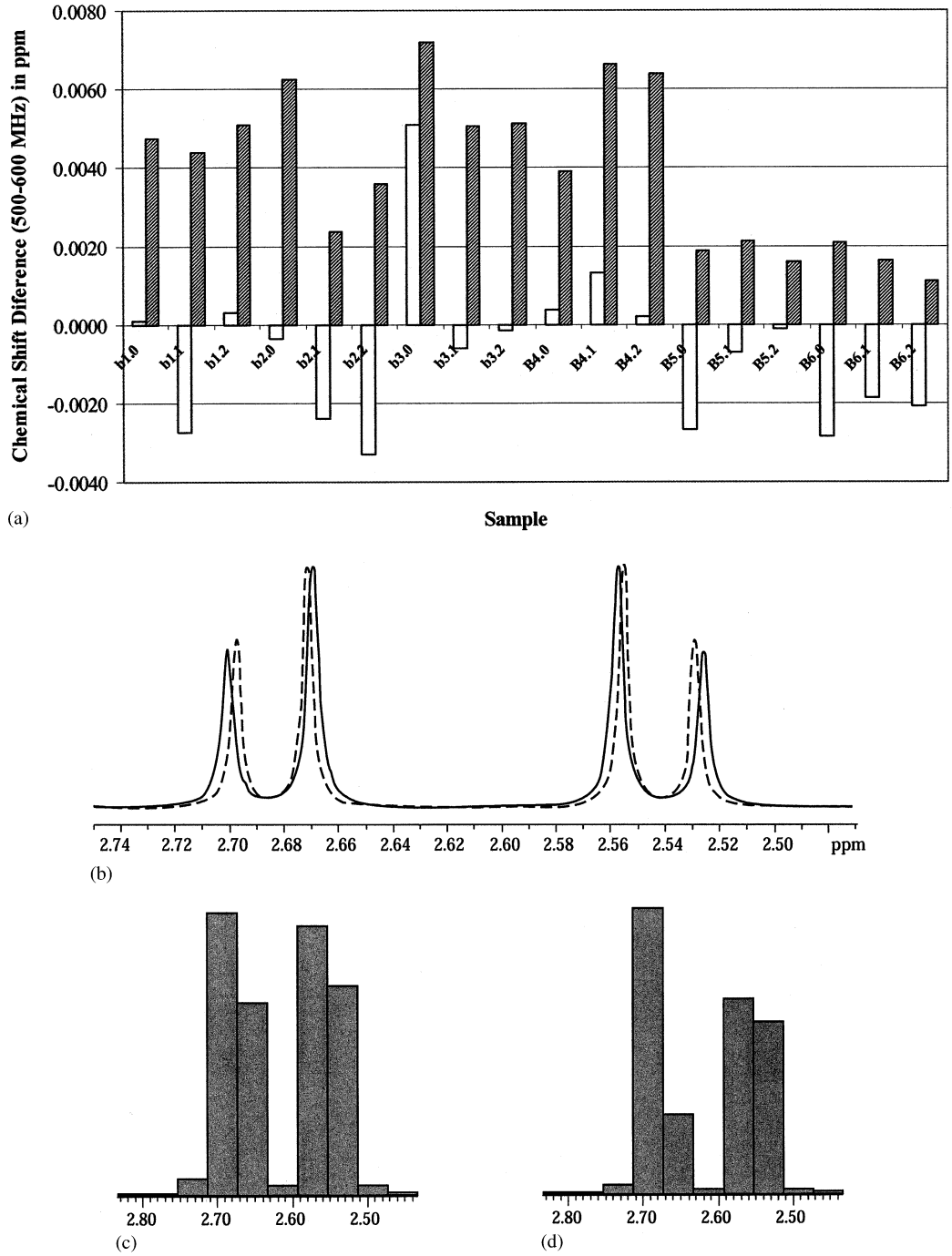

Fig. 3. (a) Citrate chemical shifts at 500 and 600 MHz were determined from the intensity-weighted average over each AB spin system. The $\Delta\delta_{(500-600\ \mathrm{MHz})}$ values are plotted for the downfield (white) and upfield (hashed) doublets. (b) The large geminal ^{2}J couplings of the citrate methylene protons (>15 Hz) can cause portions of its multiplet components to fall into different integrated segments at the two measured field strengths. Overlay of simulated 500 (solid lines) and 600 (hashed lines) MHz spectra and resulting segment analysis for the 500 (c) and 600 (d) MHz spectra. The outcome of the segment analysis is clearly dependent upon the beginning and end points of the segments, however, the segment analysis shown here is consistent with that achieved experimentally.

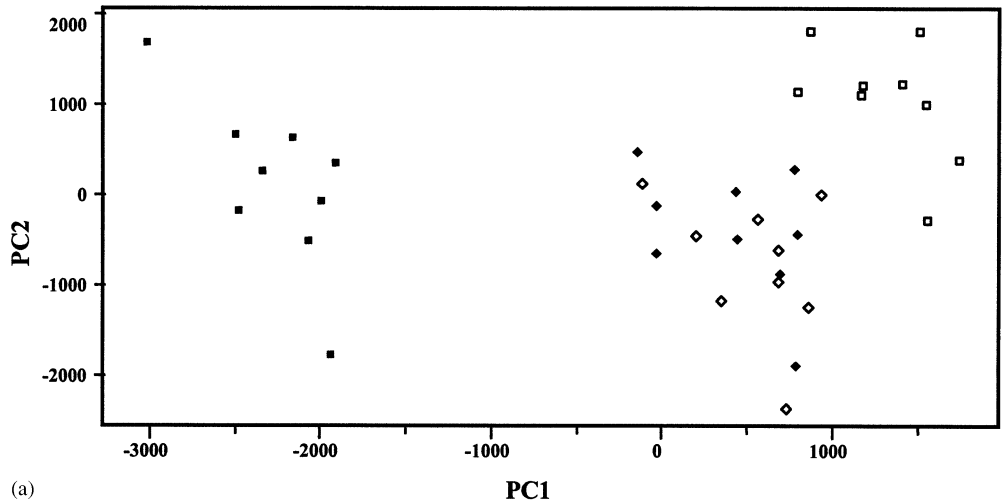

(a)

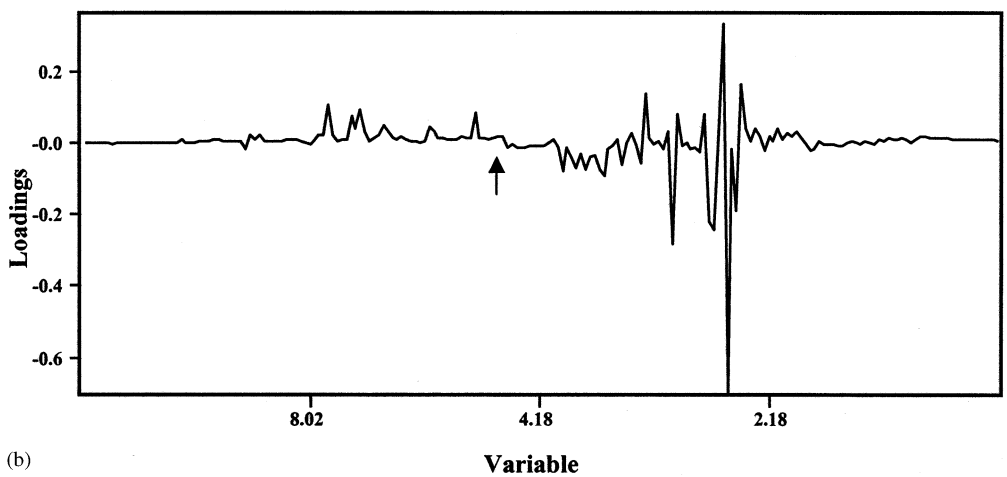

(b)

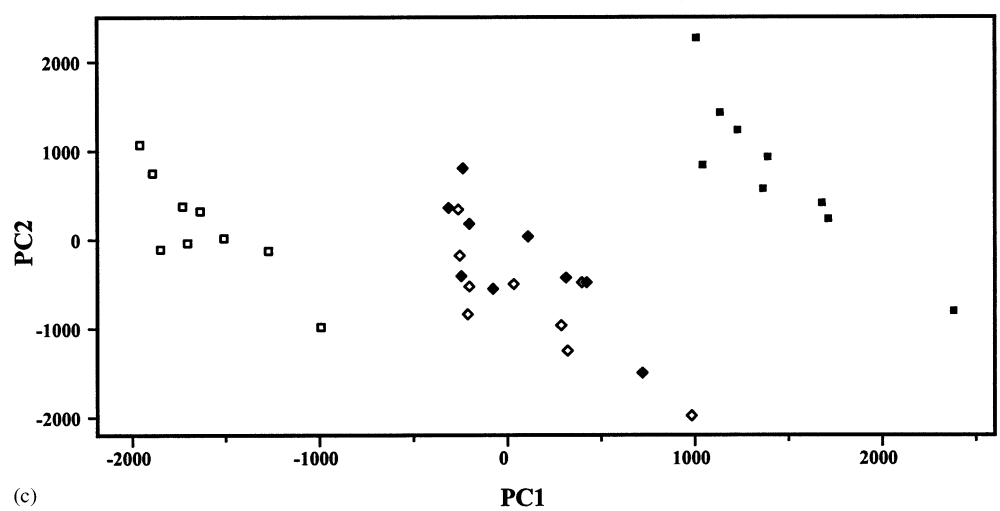

(c)

Fig. 4. PC maps (mean-centered) of low dose samples (a) and corresponding loadings for PC1 (b). Arrow denotes excluded region. PC maps regenerated after averaging across the citrate region (c) and increasing segment width to 0.07 ppm (d). Samples in PC maps are designated as follows: 600 MHz, solid squares; 500 MHz presaturation data acquired in two separate analyses, open and filled diamonds; 500 MHz Watergate, open squares.

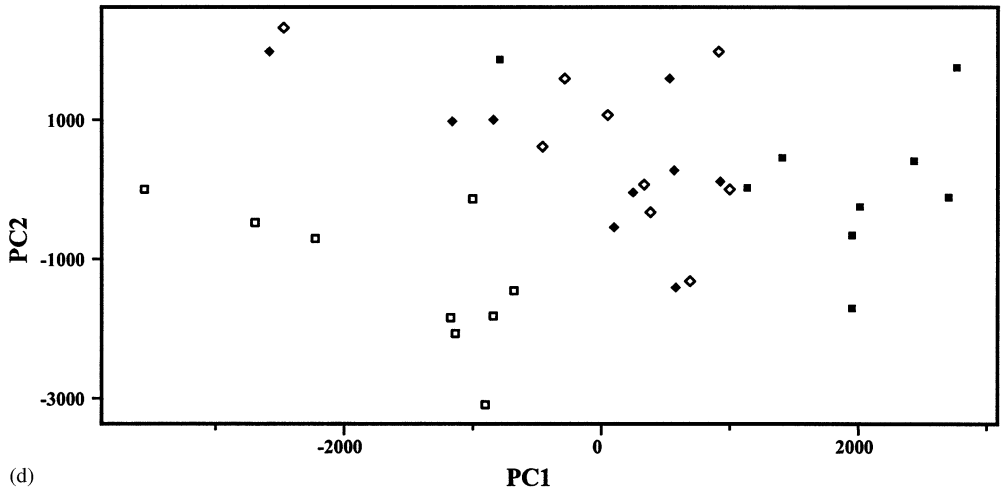

Fig. 4. (*Continued*)

spin systems with $^3J < 15$ Hz [9], the large geminal ^2J couplings of the citrate methylene protons (> 15 Hz) can cause portions of its multiplet components to fall into different integrated segments at the two measured field strengths (Fig. 3b–d). The contributions of citrate to the PC urinalysis are discussed in greater detail below.

Having established the impact of solvent suppression and general instrument-to-instrument variability relative to the BEA response, a subset of samples was selected for a more detailed comparative analysis. The low dose data (including predose) were selected in order to minimize the dose response contribution and magnify the differences between data sets. A fourth data set, representing a second acquisition of 500 MHz presaturation data obtained in a separate analysis, is included to provide an internal measure of reproducibility on the same instrument. PCA of low dose spectra collected under each of the experimental conditions were resolved in PC1, with the 600 MHz data mostly resolved from the 500 MHz data, and 500 MHz presaturation and Watergate data resolved from each other (Fig. 4a). The duplicate 500 MHz presaturation measurements showed considerable overlap, suggesting that a second freeze–thaw cycle had little effect on the samples. Line plots of the loadings for the 500 MHz low dose Watergate and presaturation spectra were similar to those obtained for the mouse presaturation/Watergate analysis, again implicating the spectral baselines as the source of resolution between these two data sets (data not shown). Several factors contributed to the resolution of the 500 and 600 MHz presaturation data on the PC map. Line plots of the loadings and spectral reconstructions of the low dose data suggested that most of the variance could be attributed to the spectral baselines, which were positively offset in the downfield region and negatively offset in the upfield region at 500 MHz compared to 600 MHz. However, the loadings indicated that citrate remained a significant source of variance between data sets; the values of the loadings were alternately positive and negative across the citrate chemical shift range (Fig. 4b). This suggested that differences in citrate chemical shifts between 500 and 600 MHz data sets, coupled with the field strength effect of similar magnitude (vide supra), were active in resolving the two data sets. By averaging the integrals across the entire citrate region (2.48–2.72 ppm), which was largely void of other metabolite signals, and employing the average value for each segment across that region, the gap between the 500 and 600 MHz data sets was effectively narrowed (Fig. 4c). A nearly identical result was achieved by removing the citrate resonances from the analysis

entirely (data not shown). Because the concentration of citrate is relatively high compared to many other metabolites, especially in the low dose samples, it could be argued that citrate is over-represented in the PC analysis. In order to give equal weight to lower concentration, albeit equally biochemically important, metabolites, PCA was performed on the full data set (predose, low dose and high dose) using autoscaling (mean-centering followed by division of each variable by its standard deviation; Fig. 2c). Unfortunately, this protocol had the undesirable effect of magnifying the differences between data sets, and while the result served to demonstrate the sensitivity of autoscaling to spectral artifacts, it also effectively corroborated the hypothesis that the baselines were a dominant source of variance between data sets.

The subtle changes in citrate chemical shifts between the 500 and 600 MHz data sets suggested differences in sample temperature, pH and/or metal ion concentrations between the two analyses. Variable temperature (VT) NMR experiments indicated that temperature alone was not sufficient to account for the observed chemical shift changes in citrate.[1] Thus, a change in metal ion concentrations and/or pH of the urine samples is implicated; the latter is consistent with previous reports of the instability of urinary pH values, even in the strongly buffered solutions [6]. The chemical shifts of other metabolite resonances are also potentially sensitive to temperature, pH and/or metal ion concentrations. A PC map generated by pooling the VT NMR data with the original data set demonstrated that variations in temperature were not a dominant source of disparity between the 500 and 600 MHz data sets (data not shown). Nevertheless, some of the existing chemical shift variability could be effectively absorbed by increasing the segment width to 0.07 ppm, which improved the clustering among data sets (Fig. 4d).

The improved clustering obtained by averaging over the citrate region (vide supra) indicated that the resolution between data sets was not due to a change in citrate concentration between analyses. However, changes in the concentrations of other metabolites were evident. Two high dose on day 1 samples showed major increases in both acetate (δ 1.95, s) and succinate (δ 2.41, s), however, the exclusion of the high dose samples from the final comparative analysis (Fig. 4) eliminated the possibility that these variations were responsible for the overall disparity between data sets. In the remaining samples, modest increases in succinate and a metabolite tentatively identified as fumarate (δ 6.59, s) were commonly observed. Removing these singlets from the PC analysis of low dose resulted in no improvement in clustering among data sets in the PC map. The general pattern consistent with microbial contamination [15] was not observed in the spectra. In fact, sodium azide was added to samples prior to the original NMR analysis at 600 MHz in an effort to prevent microbial contamination; samples were stored frozen and then thawed before analysis at 500 MHz. Nevertheless, the changes in metabolite concentrations noted above suggest that some enzymatic activity occurred between analyses during the time that samples were standing in solution. Little or no change was observed between the two 500 MHz presaturation data sets which were collected after a two week freeze–thaw cycle (Fig. 4a).

Other possible differences between the 500 and 600 MHz data sets could arise from signal-to-noise, which was approximately two times greater at 500 MHz than that achieved at 600 MHz, as measured on and around TSP. This is attributed to an increased number of scans and different probe configurations. However, the difference in signal-to-noise is unlikely to contribute appreciably to differences in the data sets since all spectra were normalized by dividing by total signal intensity over a region (0.2–10 ppm, minus excluded region) containing largely signal and little noise.

[1] Rat urine 500 MHz NMR spectra were acquired at 26°C, while 600 MHz data were acquired at ambient temperature, which apparently varied between analyses of different 96-well plates across which samples were spread. Variable temperature NMR experiments (see Section 2) established the maximum temperature difference across 600 MHz samples as 5°C. This difference results in a $\Delta\delta_{max}$ of 0.0013 ppm between citrate resonances. The maximum citrate chemical shift difference was 0.0072 ppm and occurred between two spectra that were acquired at near identical temperatures, indicating that temperature alone was not sufficient to account for the observed chemical shift changes in citrate.

In summary, several potential sources of disparity between data sets were identified, including pH, temperature, sample composition (including metal ion concentrations), signal-to-noise, field strength and spectral baselines. Among these, the greatest PC resolving power was attributed to spectral baselines and the chemical shift variability and field strength effects associated with citrate resonances. Despite all of the possible variations, the 600 MHz data clustered nicely with the 500 MHz presaturation and Watergate data in the PC1/PC2 map (Fig. 2a).

In cases where animals respond to treatment, averaging integral values across the citrate region would effectively remove both the field strength and chemical shift variability of citrate, leaving only its treatment-dependent concentration changes. While this was an effective strategy for reducing effects specifically associated with citrate and could potentially be streamlined into high-throughput mode, it cannot be guaranteed that the spectral region containing citrate will be free of other biochemically important metabolite resonances. Furthermore, the observed field strength effect is not limited to citrate, as it is conceivable that other biochemically important molecules with large couplings might arise in urine spectra. An alternative approach to addressing the field strength effect might be the utilization of F2 projections of 45°-tilted 2D*J*-resolved spectra [16,17], as adopted by Foxall et al. [9] for simplification of urine and plasma spectra. This approach would provide proton-decoupled spectra in which all of the resonances are represented by their absolute chemical shift values, and would clearly circumvent the problem of multiplet components falling into different integrated segments at different field strengths. The coupling constant data would be preserved in the second dimension and could subsequently be used to identify metabolites in the spectra. However, the additional acquisition time required to collect these data is clearly less conducive to high-throughput analysis than application of a 1D sequence. Another possible approach is the application of larger segment widths, which would be expected to reduce both the chemical shift variability and field strength effects associated with citrate and resulted in improved clustering among the three low dose data sets (Fig. 4d). However, application of increased segment widths might ultimately impede efforts to trace drug treatment-related changes in specific biomarkers present in the urine, as the larger segments give rise to poorer resolution in data reconstructed from the input descriptors.

4. Conclusions

This study demonstrated that the impact of NMR-associated variables was secondary to the apparent response to BEA treatment in the mean-centered principal component analysis of rat urine NMR spectra. The relative effect might be greater or lesser in studies of other toxins. While the overall reproducibility of the BEA treatment pattern over three NMR data sets was encouraging, the strong effect observed in PC3 suggested that instrument variability might compete with the identification of more subtle, albeit potentially important, biochemical patterns in the data that could occur as a result of toxic insult. Further limitations are suggested by the demonstration that spectral artifacts were a dominant source of variance in the autoscaled PC analysis.

Several NMR solvent suppression schemes were assessed, including Watergate, WET, presaturation, and Noesy-presat, each of which imparted unique features on the spectra. In fact, in the absence of a response to drug treatment, spectra were resolved in the PC map according to solvent suppression method. This was largely attributed to the unique baselines associated with each method and demonstrated the importance of reproducibly flat baselines in the practical application of metabonomics. With respect to the individual methods, the Watergate data were characterized by an intense residual urea signal and by signal attenuation around the residual water. This latter feature might interfere with the detection and integration of important metabolite resonances. In addition, poor phase properties around the water resonance were obtained in a subset of the spectra, even after manual optimization of the final pulse of the binomial sequence. Furthermore, it was possible to distinguish be-

tween spectra that had been acquired with different binomial 90° pulse widths (unpublished observation), suggesting another potential source of variance that might be introduced into the PC maps via the NMR. More generally, those pulse sequences requiring significant parameter optimization are more likely to introduce spectral variations that might be detected by PCA, particularly when pooling data across instruments, and are less conducive to high throughput analysis when parameter optimization is required between samples. These collective observations suggest that Watergate is not the optimal method for this application. As with Watergate, the WET sequence preserved the urea signal, however, the bulk of this signal is removed in preparation for PCA. While WET also requires some optimization, the WET spectra were generally characterized by very flat baselines, suggesting that this sequence gives rise to characteristics that might ultimately be deemed critical to metabonomics. Noesy-presat represents a robust method requiring little optimization. By minimizing the contribution from the exchangeable urea signal, the tailing of this signal and associated elevation of the baseline in the downfield region of the spectrum, as observed in the Watergate data, is eliminated. Although other exchangeable protons might be similarly attenuated, it could be argued that these protons are generally associated with molecules that are already represented in the spectra by other nonexchaneable resonances. The Noesy-presat spectra required minimal first order phase correction and baseline adjustment. A high-throughput metabonomic approach would ideally incorporate automated phase and baseline correction routines that give rise to the flattest possible baselines with minimal user intervention.

From this work, it is clear that experimental design introduces variables that can effect the outcome of NMR spectral pattern recognition. The development of methods to minimize the impact of these variables is warranted. Until such methods are in place, it is imperative that standard operating procedures for NMR data acquisition and processing be adopted as a component of a robust and universal application of metabonomics technology.

Acknowledgements

The authors gratefully acknowledge Dr Benjamin Burke for helpful discussions, Jens Knudsen for the measurement of citrate chemical shifts, and Jane Chambers for assistance with sample collection.

References

[1] J.K. Nicholson, J.C. Lindon, E. Holmes, Xenobiotica 29 (1999) 1181–1189.
[2] E. Holmes, J.P. Shockcor, Curr. Opin. Drug Disc. Dev. 3 (2000) 72–78.
[3] W. El-Deredy, NMR Biomed. 10 (1997) 99–124.
[4] M. Spraul, P. Neidig, U. Klauck, P. Kessler, E. Holmes, J.K. Nicholson, B.C. Sweatman, S.R. Salman, R.D. Farrant, E. Rahr, C.R. Beddell, J.C. Lindon, J. Pharm. Biomed. Anal. 12 (1994) 1215–1225.
[5] I.T. Joliffe, Principal Component Analysis, Springer, New York, 1986.
[6] J.C. Lindon, J.K. Nicholson, J.R. Everett, Ann. Rep. NMR Spectrosc. 38 (1999) 1–88.
[7] E. Holmes, F.W. Bonner, B.C. Sweatman, J.C. Lindon, C.R. Beddell, E. Rahr, J.K. Nicholson, Mol. Pharmacol. 42 (1992) 922–930.
[8] S. Connor, J. Everett, J.K. Nicholson, Magn. Reson. Med. 4 (1987) 461–470.
[9] P.J.D. Foxall, J.A. Parkinson, I.H. Sadler, J.C. Lindon, J.K. Nicholson, J. Pharm. Biomed. Anal. 11 (1993) 21–31.
[10] B.M. Beckwith-Hall, J.K. Nicholson, A.W. Nicholls, P.J.D. Foxall, J.C. Lindon, S.C. Connor, M. Abdi, J. Connelly, E. Holmes, Chem. Res. Toxicol. 11 (1998) 260–272.
[11] M. Liu, X. Mao, C. Ye, H. Huang, J.K. Nicholson, J.C. Lindon, J. Magn. Reson. 132 (1998) 125–129.
[12] D.G. Robertson, M.D. Reily, R.E. Sigler, D.F. Wells, D.A. Paterson, T.K. Braden, Toxicol. Sci. 57 (2000) 326–337.
[13] S.H. Smallcombe, S.L. Patt, P.A. Keifer, J. Magn. Reson., Series A 117 (1995) 295–303.
[14] V. Sklenar, M. Piotto, R. Leppik, V. Saudek, J. Magn. Reson., Series A 102 (1993) 241–245.
[15] B.C. Sweatman, R.D. Farrant, J.C. Lindon, J. Pharm. Biomed. Anal. 11 (1993) 169–172.
[16] W.P. Aue, J. Karhan, R.R. Ernst, J. Chem. Phys. 64 (1976) 4226–4227.
[17] K. Nagayama, P. Bachmann, K. Wuthrich, R.R. Ernst, J. Magn. Reson. 31 (1978) 133–148.